

LARGE-SCALE EDDIES AND THE GENERAL CIRCULATION OF THE TROPOSPHERE

ISAAC M. HELD

*Geophysical Fluid Dynamics Laboratory/NOAA
Princeton University
Princeton, New Jersey*

AND

BRIAN J. HOSKINS

*Department of Meteorology
University of Reading
Reading, England*

1. Introduction	3
2. The Hadley Cell	4
3. Rossby Wave Radiation	9
4. Eddy Flux Closure.	17
5. Stationary Eddies and Their Interaction with Transients	20
5.1. Extratropical Stationary Eddies	20
5.2. Tropical Stationary Eddies	23
5.3. Zonally Asymmetric Transients	26
References	29

1. INTRODUCTION

Our theoretical understanding of the general circulation of the atmosphere, and of the role of large-scale eddies in maintaining that circulation, is primitive but rapidly evolving. There exist several interesting ideas relevant to closure schemes for mid-latitude eddies generated by baroclinic instability, but none is so well founded in theory as to be convincing, and systematic tests against eddy-resolving numerical models are as yet very limited. There is a substantial body of work on weakly nonlinear baroclinic waves, but its relevance for the atmosphere remains obscure. A host of competing theories have been proposed recently to explain the distinctive structure of the low-frequency variability of the atmosphere. Analyses of observations and general circulation models are evolving particularly rapidly and complementing each other as they focus on the most dynamically interesting budgets and statistics. And new global data sets are making possible meaningful studies of dynamical balances in the tropics and of planetary wave propagation between the tropics and mid-latitudes. Our reaction to this turbulent state of

affairs is to present our own idiosyncratic views on how different parts of the system fit together and on what some of the outstanding problems are. If there is any theme to be found beneath the surface of this essay, it may be the following: in developing general circulation theory and eddy flux closures, we must move beyond speculation followed by qualitative comparison with the atmosphere in all its complexity, toward formulating hypotheses that can be quantitatively tested against idealized numerical models designed for the purpose. As evidence that this approach is feasible, we have the remarkable success of numerical general circulation models (GCMs) of the atmosphere, to which Dr. Smagorinsky has made such a decisive contribution. We are delighted to contribute this essay to a book honoring his achievements.

2. THE HADLEY CELL

Until stated otherwise, we consider an atmosphere with zonally symmetric lower boundary conditions and external forcing and, therefore, a zonally symmetric climate. Fortunately, experiments with GCMs indicate that the climate of such an atmosphere does not differ greatly from the zonal average of the climate produced by realistic Earth-like asymmetries in the lower boundary. We begin by asking what form the general circulation might take in the absence of “large-scale” eddies, keeping in mind that if one somehow suppresses the baroclinic and barotropic instabilities primarily responsible for cyclone- and planetary-scale eddies, small-scale eddies will still be generated in the surface boundary layer and by gravitational and, perhaps, inertial or Kelvin – Helmholtz instabilities in the free atmosphere.

Take the vertical temperature and moisture structures as given for the moment, so as to isolate problems associated with horizontal temperature gradients and vertical wind shears. In the absence of any time-mean flow, suppose that radiation plus convection produce the temperature field $T_E(\theta, p)$. In a rapidly rotating atmosphere, one is tempted to set $T = T_E$ as a first approximation, assume thermal wind balance,

$$f[\partial u / \partial \ln(p)] = (R/a)(\partial T / \partial \theta) \quad (2.1)$$

and then obtain the wind field by assuming that surface drag is sufficient to maintain $u \approx 0$ near the surface. Unless one is so fortunate that $\partial T_E / \partial \theta$ is identically zero at the equator, this procedure is clearly inadequate, since the resulting wind will be infinite at the equator. Difficulties remain even if T_E happens to be symmetric about the equator, as the following heuristic model [based on Held and Hou (1980)] demonstrates. The model also suggests how axisymmetric large-scale flow in the tropics (the Hadley cell) corrects these deficiencies.

Assume that the meridional flow is confined (as it is in the Hadley cell) to two boundary layers at the surface, $p = p_s$, and at the tropopause, $p = p_T$, of pressure thicknesses δ_s and δ_T . Define a mass transport velocity $V = v_T \delta_T / \Delta p = -v_s \delta_s / \Delta p$, where v_s and v_T are the meridional velocities averaged over each layer and $\Delta p = p_s - p_T$. A thermodynamic equation adequate for our purposes is

$$0 = -\nabla \cdot (mv) - c_p(T - T_E)/\tau \quad (2.2)$$

where m is the moist static energy, $c_p T + gz + Lr$, τ is a radiative relaxation time, and $v = (v, \omega)$. Vertically integrating, we have

$$[T] = [T_E] - \frac{\tau}{a \cos(\theta)} \frac{\partial}{\partial \theta} (\cos(\theta) S V) \quad (2.3)$$

where

$$[T] \equiv \frac{1}{\Delta p} \int_{p_T}^{p_s} T dp \quad (2.4)$$

while

$$S \equiv [m(p_T) - m(p_s)]/c_p \quad (2.5)$$

is a measure of the gross moist stability of the atmosphere. Here $[T]$ can be related to $u(p_T) = U$ by vertically integrating (2.1) and assuming that $u(p_s)$ is negligibly small,

$$fU = -\frac{R}{a} \frac{\partial}{\partial \theta} \int T d \ln(p) \quad (2.6)$$

Assuming further that the vertical profile of T is independent of latitude, $T = [T](\theta) + t(p)$, then

$$fU = -\frac{R\chi}{a} \frac{\partial [T]}{\partial \theta} \quad (2.7)$$

where χ is the depth of the troposphere in scale heights. A relation between U and V must be obtained from the zonal angular momentum budget. In the spirit of constructing a simple heuristic model, we assume that angular momentum is conserved following a horizontal streamline at the top of the Hadley cell, except for linear damping:

$$\kappa U = (f + \zeta)V = -\frac{V}{a^2 \cos(\theta)} \frac{\partial M}{\partial \theta} \quad (2.8)$$

where $M = \Omega a^2 \cos^2(\theta) + Ua \cos(\theta)$, ζ is the relative vorticity, and κ is a constant. We now have three equations [(2.3), (2.7), and (2.8)] in the three

unknowns U , V , and $[T]$. The only nonlinearity results from the advection of relative vorticity in (2.8). Similar models have been discussed by Hou (1984) and Schneider (1983).

Assuming that $\kappa \neq 0$, (2.8) implies that $U = 0$ at the point of maximum angular momentum. Therefore, $M \leq \Omega a^2$ at all latitudes. Equivalently, $U(\theta) \leq U_M(\theta) = \Omega a \sin^2(\theta)/\cos(\theta)$. Returning to (2.8), we see that as $\kappa \rightarrow 0$, either V or $f + \zeta$ must vanish. But in regions where $V \rightarrow 0$, we also must have $[T] \rightarrow [T_E]$ and $U \rightarrow U_E$ where U_E is the wind field in balance with $\partial[T_E]/\partial\theta$. Therefore, wherever $U_E > U_M$, $f + \zeta$ must vanish as $\kappa \rightarrow 0$. Figure 1a shows the zonal winds produced by this model for several values of the parameter $\kappa S\tau$. (U is a function of κ , S , and τ only through the combination $\kappa S\tau$.) Also plotted are U_E and U_M . Here $[T_E]$ is symmetric about the equator; its form and the values of the other model parameters are given in the figure caption. Figure 1b shows the absolute vorticities corresponding to the winds in Fig. 1a. As analyzed in Held and Hou (1980), the region in which the absolute vorticity vanishes as $\kappa \rightarrow 0$ is somewhat larger than that in which $U_E > U_M$. The results are qualitatively similar if the forcing is asymmetric about the equator; the region within which $f + \zeta \rightarrow 0$ is then asymmetric as well.

If large-scale eddies were suppressed, what processes would result in significant stress on the upper-tropospheric flow in the Hadley cell? It has been

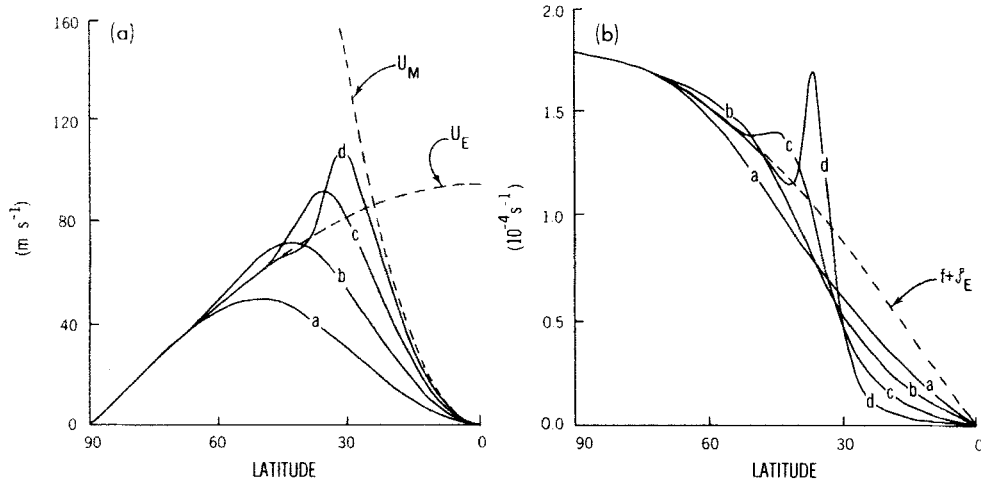


FIG. 1. (a) Zonal wind and (b) absolute vorticity as function of latitude predicted by the idealized Hadley cell model of Section 2. The radiative equilibrium temperature $[T_E]$ is set equal to $T_0(1 - \Delta_H P_2[\sin(\theta)])$ with $\Delta_H = \frac{1}{3}$. T_0 is chosen so that $R\chi T_0/g = 15$ km, and P_2 is the second Legendre polynomial. The curves a-d correspond to the four values of the parameter $\kappa S\tau = (0.3, 0.075, 0.015, 0.003)T_0$. Also shown are the angular momentum conserving wind U_M and the radiative equilibrium wind U_E .

suggested [e.g., Holton and Colton (1972), Schneider and Lindzen (1976), Chang (1977)] that momentum fluxes in cumulus convection are significant in this regard. Our view at present is that such fluxes are unlikely to be important for the planetary-scale flow since (1) there is little deep convection in regions of large vertical shear where the mixing would have relatively large effects on the flow field [see Thompson and Hartmann (1979)], (2) GCMs that do not include this “cumulus friction” are not grossly in error in their climate simulations [e.g., Manabe *et al.*, (1974)], (3) it is not clear that the momentum fluxes would be systematically of one sign — if the convection is organized two-dimensionally, linear theory leads one to expect countergradient momentum fluxes [see Lemone (1983) for an interesting observational study of the momentum fluxes due to a tropical squall line], and (4) diagnosis of the upper-tropospheric vorticity budget from data collected at the European Centre for Medium Range Weather Forecasts (ECMWF) does not suggest a large residual in the frictionless vorticity equation [Sardeshmukh and Hoskins (1984); also Section 5 below]. Our hypothesis is that the limit of small κ is appropriate in (2.8).

The important implication of these arguments is that a very strong and sharp subtropical jet would exist if large-scale eddies were suppressed. One of the most important roles played by these eddies is, therefore, that of providing stresses that prevent the poleward flow in the Hadley cell from conserving angular momentum. Furthermore, in the absence of these stresses, the absolute vorticity equatorward of the jet would be small (Fig. 1b). It appears that the large-scale eddies help to maintain the tropical upper-tropospheric vorticities and vorticity gradients, and since these gradients are essential for the propagation of extratropical planetary waves into the tropics, the potential for interesting wave–mean flow interaction certainly exists.

The vertical structure of the tropical atmosphere enters the model [(2.3), (2.7), (2.8)] through the tropopause height and the stability parameter S . Of these, the former is the easier to understand to a first approximation. Indeed, a simple way of estimating the tropical tropopause height is to couple the rule that $S \approx 0$, i.e., that the moist static energy in the upper branch of the Hadley cell is comparable to that in the surface layer, with a radiative–convective model with prescribed clouds and relative humidity [e.g., Manabe and Wetherald (1967)]. The radiative–convective model provides one relation between the tropospheric lapse rate and the tropopause height, and the rule $S \approx 0$ another [see Held (1982) for details]. Of course, this scheme should ideally be replaced by a theory for the vertical distribution of the convective heating, as well as of relative humidity and cloudiness.

In our simple tropical model, the key dynamical quantity is the stability parameter S , which may be small but must be positive if the Hadley cell is to carry energy poleward. The factors that control S , or the closely related

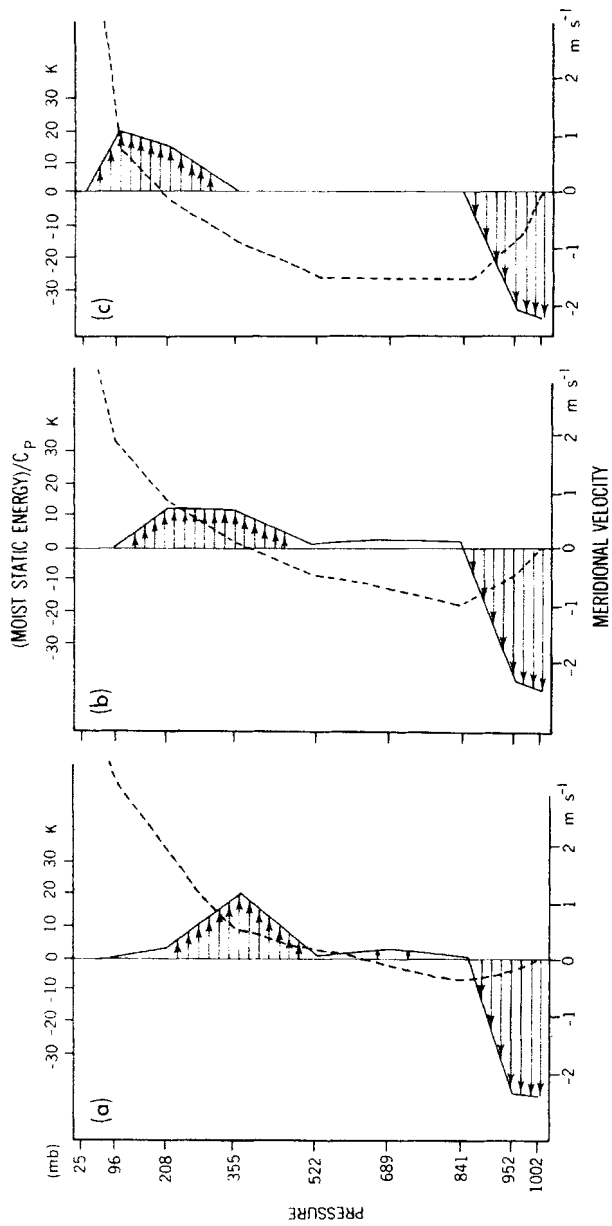


FIG. 2. Meridional wind (arrows) and moist static energy profile $m(p) - m(p_s)$ as functions of pressure at the latitude of maximum mass transport in the Hadley cell, for three different values of the solar constant: (a) 10%, (b) 0%, (c) 10%.

degree of compensation between the oppositely directed horizontal fluxes of dry static energy and latent heat in the Hadley cell, remain obscure to us. Figure 2 describes some preliminary results from an idealized numerical general circulation model, forced by annual mean insolation and with a “swamp” (flat, zero heat capacity, water-saturated surface) as lower boundary. Three experiments were performed — one with the standard value of the solar constant and two others with the solar constant increased and decreased by 10%. Surface albedos and cloud amounts were held fixed. There are nine levels in the vertical, and convection is treated with Manabe’s convective adjustment scheme. The figure shows the vertical profile of moist static energy $m(p)$ (subtracting off the value of m at the lowest model level) and of meridional velocity $v(p)$ in the three cases, at the latitude of maximum mass transport in the Hadley cell (12° latitude in each case). Clearly evident is the increase in conditional instability of the atmosphere as it warms and the increase in height of the poleward flow required to maintain $S > 0$. While the changes in mass transport are small (the mass transport is set equal to $\int v dp$, with the integral from the surface to the level at which v changes sign), the dry static energy flux increases dramatically with increasing insolation because of the increased height of the poleward flow. However, there is greater compensation between dry static energy and latent heat fluxes: $-(\text{latent heat flux})/(\text{dry static energy flux}) = (0.67, 0.72, 0.83)$ in the $(-10\%, 0, +10\%)$ calculations. As a result, S remains almost constant: $S = (\text{moist static energy flux})/(c_p \times \text{mass flux}) = (13.3, 15.9, 13.4 \text{ K})$. We have no arguments at present for the constancy of S or of its value of $\approx 15 \text{ K}$ in these calculations. The dependence of S on the convective parameterization and boundary layer schemes in GCMs deserves careful examination.

The problem is complicated further by the importance of the latitudinal dependence of S for the structure of the flow. From Eq. (2.3), we see that if V is to have sharp gradients, as it must at an Intertropical Convergence Zone (ITCZ), then S must also have sharp gradients, for $[T]$ is constrained to be smooth by (2.7) and (2.8). These sharp gradients in S can only come from the low-level moisture field. That structure in the moisture field is of such importance makes the construction of idealized Hadley cell models particularly challenging.

3. ROSSBY WAVE RADIATION

The dynamics of the stratosphere and mesosphere is controlled to a great extent by planetary waves excited in the troposphere. Much has been learned by specifying the tropospheric sources and concentrating instead on the wave propagation into the middle atmosphere and on the ultimate fate, or “dissipation” of these waves, with particular regard to the irreversible mixing

induced in the process [e.g., Matsuno (1971), Holton and Lindzen (1972), McIntyre and Palmer (1984)]. While there are limitations to this approach if the stratospheric dynamics feeds back significantly on the wave source [as in Plumb's (1981) idealized sudden warming model, for example], it has certainly proven to be fruitful. We believe that a similar approach is fruitful when analyzing large-scale tropospheric dynamics, important wave sources being baroclinic instability in the lower troposphere in middle and high latitudes, and deep convective heating in the tropics.

The basic assumption of this approach when applied to baroclinic instability is that irreversible mixing due to these instabilities can be divided into two distinct parts: that in the source region near the surface in mid-latitudes and that in the region where the planetary waves are "dissipated." This picture is suggested by the calculations of baroclinic wave "life cycles" described in Simmons and Hoskins (1978, 1980) and further discussed by Edmon *et al.* (1980), Hoskins (1983), and Hoskins and McIntyre (1985). Having specified a zonal flow on the sphere, the most unstable normal mode for a particular wave number M is determined. An integration of a nonlinear model including zonal wave numbers M , $2M$, $3M$, etc., is then initialized with the zonal flow plus a small amplitude normal mode. We confine the discussion here to the $M = 6$ mode for the basic flow of Simmons and Hoskins (1980), as the behavior is typical of that obtained for long wavelengths. Linear theory applies for the first few days, with eddy energy levels growing approximately exponentially at all heights. As the low-level temperature wave amplitude becomes large, there is a tendency to frontogenesis and a decrease in growth rate of the low-level energy, until at day 5–6 the eddy occludes and low-level growth ceases. It is during this period that the most significant low-level heat transfers occur. The westward tilt in the troposphere is maintained and the upper-level energy continues to grow until about day 7.5. At this stage, the upper-level troughs develop a large SW to NE tilt on their equatorward side. There are very large poleward transports of westerly momentum, and the eddy kinetic energy is almost completely converted into zonal kinetic energy.

The same baroclinic wave life cycle can be described, following Edmon *et al.* (1980), by using wave propagation and potential vorticity concepts. For a small-amplitude perturbation to a zonal flow the linearized, frictionless quasi-geostrophic potential vorticity equation may be written

$$\frac{\partial q'}{\partial t} = -\bar{u} \frac{\partial q'}{\partial x} - v' \frac{\partial \bar{q}}{\partial y} \quad (3.1)$$

Multiplying by q' , taking the zonal average and dividing by $\partial \bar{q} / \partial y$ gives

$$\frac{\partial A}{\partial t} = -\overline{v'q'} = -\nabla \cdot \mathbf{F} \quad (3.2)$$

where

$$A = \frac{1}{2} \frac{\overline{q'^2}}{\partial \bar{q} / \partial y} = \frac{1}{2} \overline{\eta'^2} \frac{\partial \bar{q}}{\partial y} \quad (3.3)$$

is a measure of the wave activity, $\eta' = -q' / (\partial \bar{q} / \partial y)$ is the meridional particle displacement, and

$$\mathbf{F} = (-\overline{u'v'}, \frac{f_0}{N^2} \overline{v'\Theta'}) \quad (3.4)$$

is the Eliassen–Palm (EP) flux vector (Andrews and McIntyre, 1976; Edmon *et al.*, 1980). When the concept of group velocity is applicable and when waves having only one value of the group velocity \mathbf{c}_g are present, $\mathbf{F} = \mathbf{c}_g A$. For $\partial \bar{q} / \partial y$ positive, it follows from (3.2) that net propagation of wave activity into a region as shown by convergence of the EP flux implies a down-gradient potential vorticity flux, an increase in the q variance along a line of latitude, and increased latitudinal dispersion of fluid particles originally located at that latitude. In the absence of dissipation, the sign of all of these quantities is reversed as the wave activity propagates out of the region. The mean flow potential vorticity equation reduces to

$$\frac{\partial \bar{q}}{\partial t} = - \frac{\partial}{\partial y} \overline{v'q'} \quad (3.5)$$

Boundary temperature equations of the forms (3.1) and (3.5), with Θ' replacing q' , are then needed to complete the eddy and mean flow problems.

The applicability of quasi-geostrophic theory to a situation in which the static stability varies greatly across a sloping tropopause and in which the relative vorticity is comparable with the Coriolis parameter in some regions is dubious; however, (3.1) is valid for the Ertel potential vorticity perturbation on isentropic surfaces and analogs of (3.2)–(3.4) exist. For nonlinear large-amplitude waves the simplicity of the preceding equations is lost; we assume that they may still be used as guidance in the diagnosis of the dynamical processes involved. The following discussion is a shortened version of that given in Hoskins and McIntyre (1985).

A schematic picture of the EP flux \mathbf{F} at three different stages in the life cycle is given in Fig. 3. The detailed pictures for this and $\partial \bar{q} / \partial y$ are given in Hoskins (1983). Initially \mathbf{F} is almost vertical and confined to low levels. As the low-level growth decreases, the arrows become large in the middle troposphere and have strong convergence at upper-tropospheric levels, implying vertical propagation of wave activity. By day 8 this process is complete and the arrows now point quasi-horizontally beneath the sloping tropopause; there is divergence near 50°N and 350 mb where before there had been convergence, and strong convergence near 30°N and 150 mb. The picture in

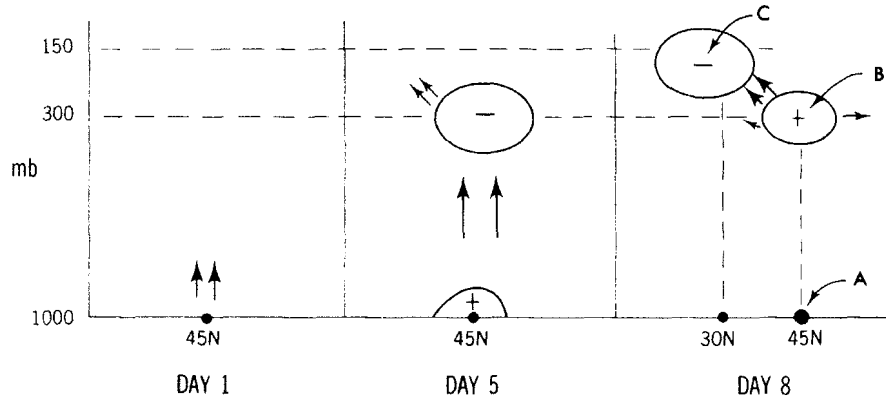


FIG. 3. Schematic of the Eliassen-Palm flux (arrows) and divergence of this flux (contours with plus or minus sign) at three times during the baroclinic eddy life-cycle calculation described in Section 3. The points A (45° , 1000 mb), B (45° , 300 mb), and C (30° , 150 mb) are referred to in the text and in Fig. 4.

this stage is of quasi-horizontal propagation from mid-latitudes into the subtropics.

To add substance to this picture, estimates of particle dispersion have been computed for the three points shown in Fig. 3. For point A, near the surface at 45°N , vertical advection is negligible in the thermodynamic equation and η' can be obtained from the temperature distribution. We define $\tilde{\eta}$ to be the maximum latitudinal excursion of the temperature contour centered at the latitude of interest. Curve A in Fig. 4 shows the time evolution of $\tilde{\eta}$ at point A. The temperature field at this level on day 6, following several days of almost exponential growth in $\tilde{\eta}$, is shown in Fig. 5a. The frontogenesis and occlusion process have left only a very narrow region of warm air at 45°N . This region is eroded by the term representing sub-grid-scale mixing in the model until, by day 8, the isotherm displacement is near zero. Because of the mixing processes that have come into play, however, $\tilde{\eta}$ cannot be used as a measure of particle dispersion beyond day 6.

The curves for points B and C are both obtained from the maximum latitudinal excursions on isentropic surfaces of the Ertel potential vorticity contour centered at the point of interest. At point B, the growth of $\tilde{\eta}$ lags that at A. It reaches a maximum soon after day 7 and declines to negligible values at day 10. Analysis shows the dynamics here to be nearly reversible, with fluid particles returning to their initial latitudes. The growth of $\tilde{\eta}$ at C slightly lags that at B but continues until day 8. The Ertel potential vorticity on the 350-K isentropic surface (which passes close to C) is illustrated in Fig. 5b. The potential vorticity field is being wrapped around a large subtropical gyre. This wrapping, or "wave breaking," continues and generates small-scale

structures that are eventually dissipated. There is a marked similarity between these processes and those noted by McIntyre and Palmer (1984) as occurring in the stratosphere.

A simple model that provides a hint of the wave behavior responsible for the last stage of this life cycle is the nondivergent barotropic vorticity equation on the sphere, linearized about a zonal-mean zonal flow \bar{u} :

$$\frac{\partial \zeta'}{\partial t} = -\frac{\bar{u}}{a \cos(\theta)} \frac{\partial \zeta'}{\partial \lambda} - \frac{\gamma}{a \cos(\theta)} \frac{\partial \psi'}{\partial \lambda} + \nu \nabla^2 \zeta' \quad (3.6)$$

where $\gamma = a^{-1} \partial(f + \bar{\zeta})/\partial\theta$. The resulting mean flow accelerations can be computed from

$$\frac{\partial \bar{u}}{\partial t} = \overline{v' \zeta'} = -\frac{\partial}{\partial t} \frac{\overline{\zeta'^2}}{2\gamma} - \nu \frac{\overline{|\nabla \zeta'|^2}}{2\gamma} \quad (3.7)$$

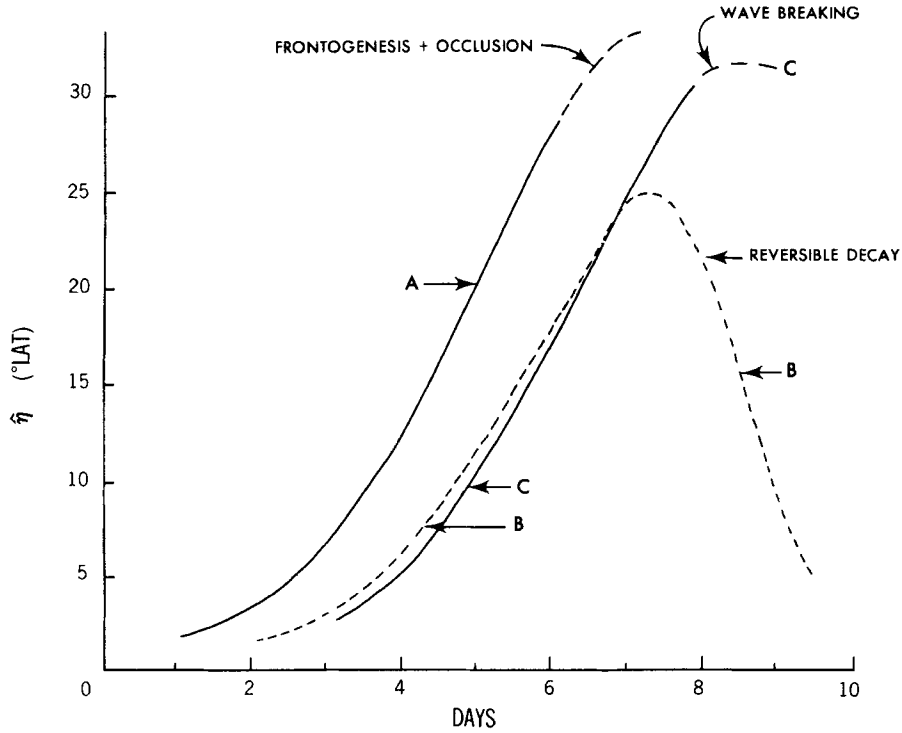


FIG. 4. Maximum meridional displacement of fluid particles (in degrees of latitude) initially at the points A, B, and C of Fig. 3, for the baroclinic eddy life-cycle calculation, estimated as described in the text.

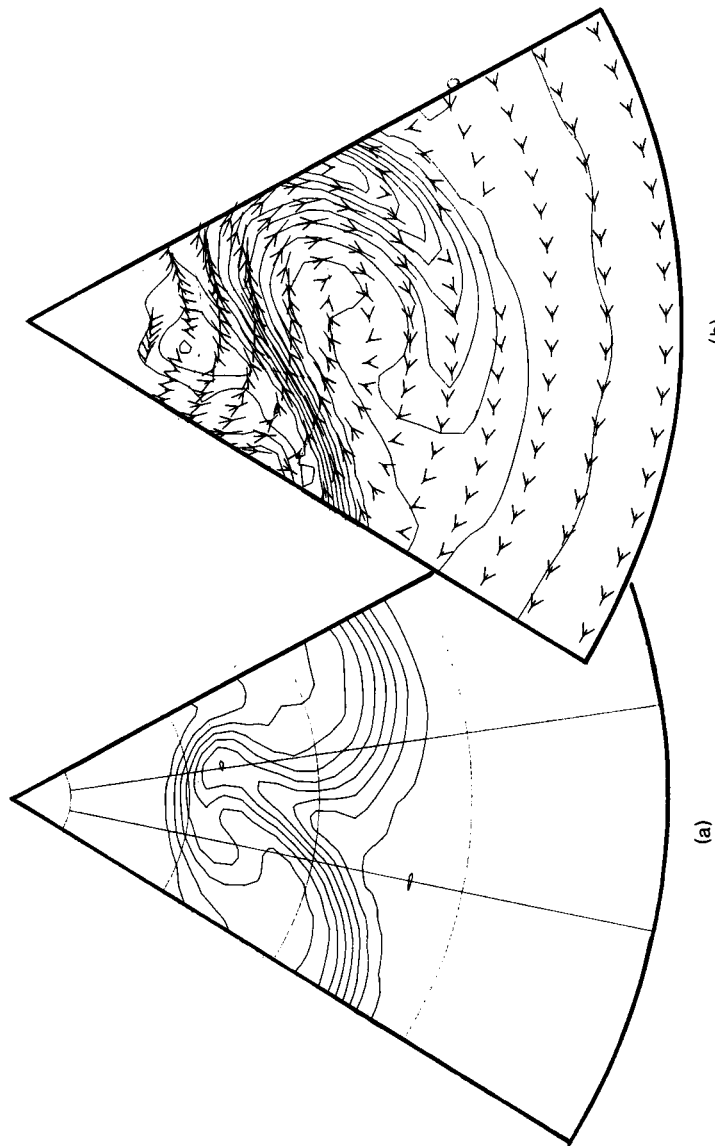


FIG. 5. (a) Temperature field on the lowest sigma-surface (0.967) at day 6 of the life cycle calculation and (b) Ertel potential vorticity field on the 350-K isentropic surface at day 8. The contour intervals are 5 K and $0.8 \times 10^{-6} \text{ m}^2 \text{ s}^{-1} \text{ K kg}^{-1}$ and the arrows in (b) are the flow field on this isentropic surface, in a frame of reference moving with the phase speed of the wave.

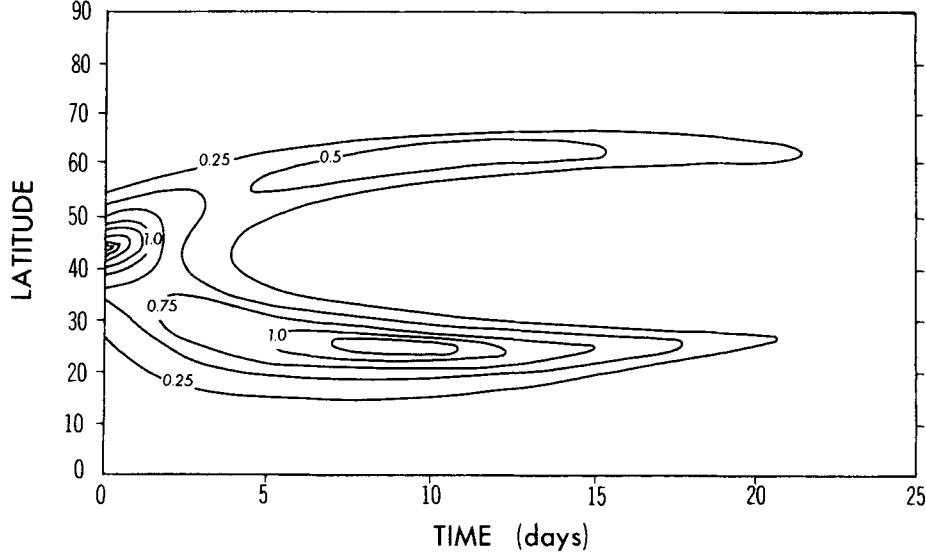


FIG. 6. Evolution of wave activity in the linear barotropic decay calculation described in the text. Contour interval is 0.25 m s^{-1} .

but we do not take these changes in mean wind into account in the linear model described here. In Figs. 6 and 7 we show the result of integrating (3.6) from the initial condition

$$\zeta'(\theta, \lambda) = C \cos(\theta) \cos(M\lambda) \exp\{-[(\theta - 45^\circ)/10^\circ]^2\} \quad (3.8)$$

with $M = 6$ and $C = 5.0 \times 10^{-5} \text{ s}^{-1}$. Plotted in Fig. 6 is the evolution of the wave activity

$$A = \frac{\overline{\zeta'^2} \cos(\theta)}{2\gamma} \quad (3.9)$$

assuming a wind profile typical of that in the wintertime upper troposphere, given by

$$\bar{u}(\theta) = (18 \text{ m s}^{-1}) \sin\{(3\pi/2)[1 + \sin(\theta)]\} + (14 \text{ m s}^{-1}) \cos^2(\theta) \quad (3.10)$$

and setting $\nu = 10^4 \text{ m}^2 \text{ s}^{-1}$. As can be seen from (3.7), the domain integral of A is conserved in the absence of dissipation. Choosing a time T large enough that the eddy activity at this time is negligible, we can compute from (3.7) the net change in mean zonal wind induced by the eddy propagation and decay as

$$[\bar{u}(T) - \bar{u}(0)] \cos(\theta) = A(t=0) - \frac{\nu}{2\gamma} \int_0^T \overline{|\nabla \zeta'|^2} dt \cos(\theta) \quad (3.11)$$

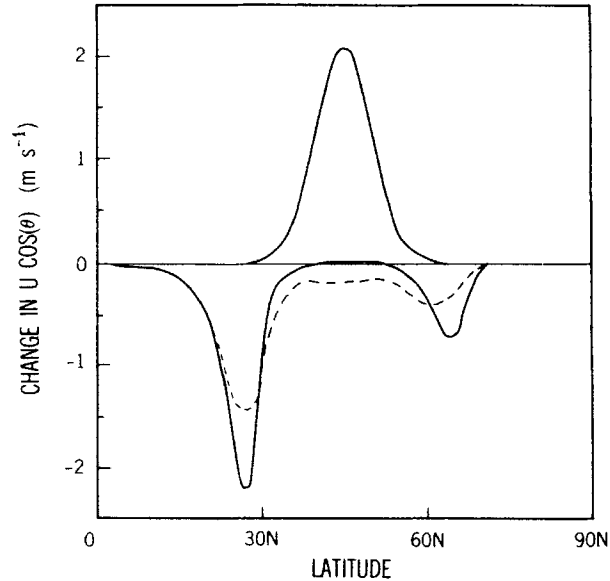


FIG. 7. Final zonal-mean flow modification predicted by linear barotropic model of Fig. 6 for two different diffusivities. The solid line above the axis is the mean flow acceleration due to the radiation of wave activity out of the region where it was initially located [the first term on the right-hand side of (3.11)]; the lines below the axis are the mean flow decelerations (for the two values of ν) due to the dissipation of wave activity [the second term on the right-hand side of (3.11)]. (—, $\nu = 10^4 \text{ m}^2 \text{ s}^{-1}$; - - - - , $\nu = 10^5 \text{ m}^2 \text{ s}^{-1}$.)

The two terms on the right-hand side, and their sum, are plotted in Fig. 7 for $\nu = 10^4$ as well as for the larger value of 10^5 .

In the case of solid body rotation (not shown), the eddy activity spreads more or less uniformly over the sphere. The mean flow is accelerated in the region in which the initial wave activity is large, while the compensating deceleration, determined by the dissipation of wave activity, occurs over a wide range of latitudes. For the typical wintertime profile, however, the wave drag is focused in subtropical and, to a lesser extent, subpolar latitudes. This behavior can be understood qualitatively by thinking of the initial disturbance as being made up of a number of wave packets with different dominant meridional wave numbers and, therefore, different phase speeds c . For $M = 6$, all of these wave packets have critical latitudes where $\bar{u} = c$ and are absorbed as they approach these latitudes [see, e.g., Yamagata (1976)]. (For longer waves, $M = 1-3$, the initial condition would also contain wave packets with phase speeds that are westward with respect to the mean flow at all latitudes; the evolution of this part of the initial condition would resemble more closely that found in the case of solid body rotation.) The linear model generates a cascade to small meridional scales near where the dominant wave

packets in the initial disturbance reach their critical latitudes and near where one also expects the fully nonlinear model to wrap the vorticity contours so as to ultimately dissipate enstrophy.

This linear model captures the basic mechanism, Rossby wave dispersion out of mid-latitudes, that generates the eddy momentum fluxes in the atmosphere. These eddy momentum fluxes determine the surface stress and, therefore, the surface wind distribution outside of the deep tropics, since the convergence of the eddy flux in these regions can only be balanced in the time mean by surface drag. We say *determine* rather than simply *balance* the surface stress, since it is difficult to see how the small surface winds have a significant back effect on the wave sources if the surface is uniform. (In the presence of surface orography there are significant feedback possibilities of this sort, however.) Note also that the initial condition in this calculation has no meridional phase tilt. If we loosely think of baroclinic instability as creating the initial disturbance, it is evident that the momentum fluxes generated by the wave dispersion need bear no close resemblance to the momentum fluxes associated with the structure of the unstable wave.

It is clear from linear results such as these, as well as the life-cycle studies and observational analyses, that the tropical upper troposphere is a graveyard for planetary wave activity. The mixing induced by this wave dissipation is, as we have argued in Section 2, crucial in determining the zonal wind and vorticity gradient profiles in low latitudes. Since there does seem to be a region (point B in Fig. 4) where the dynamics is nearly linear and reversible, we believe that much can be done in studying this upper-tropospheric mixing by ignoring the complexities of the mixing in the source region and instead specifying the wave sources. Simplification of this sort is needed to help make sense of the complex of questions associated with the interaction of equatorward propagating planetary waves with the zonal flow, the Hadley cell, and moist convection in the tropics.

4. EDDY FLUX CLOSURE

One can conceive of an eddy flux closure scheme based on the ideas of the preceding section as consisting of two parts: a theory of finite amplitude baroclinic instability that provides not only the irreversible mixing in the source region in mid-latitudes near the surface but also the space-time spectrum of planetary waves radiating out of this region; plus a theory of mixing induced by these waves after their propagation into the subtropics or the middle atmosphere. Whether or not this separation of the mixing into two distinct parts is useful, our view is that nearly all of the mixing is the end result of a cascade process, with the rate of dissipation of potential enstrophy

in the interior (or temperature variance near the lower boundary) controlled by the large scales themselves, as in fully developed turbulence. This “strongly nonlinear” picture should be contrasted with “weakly nonlinear” theories in which this rate of dissipation is determined by the strength of radiative damping, Ekman pumping, or thermal interchange with the surface.

Specifically, the time-averaged quasi-geostrophic potential enstrophy budget reads $\{v'q' \partial \bar{q} / \partial y\} = \{\text{dissipation}\}$, where braces denote a horizontal average and the overbar a time mean. The mean flow modification resulting from the eddy potential vorticity flux is thus intimately related to the enstrophy dissipation. In a “weakly nonlinear” theory, one has, schematically, $\{\text{dissipation}\} = \mu \langle q'^2 \rangle$, with μ independent of the large-scale flow, and the potential enstrophy production and dissipation both occur on the same large scales. Examples of “weakly nonlinear” theories can be found in several papers by Pedlosky (1970, 1979). The simple scaling arguments of Stone (1972) and Held (1978) for the magnitude of the transient fluxes in the source region should be thought of as “strongly nonlinear,” since the claim made is that these magnitudes can be understood to first approximation without explicit reference to the strength of radiative damping, Ekman pumping, etc., and this is only possible if dissipation rates are determined by cascade rates.

This issue could, in theory, be settled by observational analyses, although the difficulty of obtaining a well-balanced potential enstrophy budget for transient eddies in the tropospheric interior or for temperature variance near the surface suggests that GCMs may be required for this purpose. It may well be that compromise is necessary, with cascades to small scales and dissipation on the large scale both being of importance. We suspect that such a compromise is more likely to be needed near the surface; on the one hand, the cascade of temperature variance is evident in the occlusion and frontal formation processes; on the other hand, it is likely that air-mass modification through heat exchange with the surface also plays a significant role, particularly over the oceans.

A proposal for mixing by baroclinic instabilities in the source region that has attracted considerable attention is that of “baroclinic adjustment” (Smagorinsky, 1963; Stone, 1978). In analogy with the well-known treatment of mixing due to gravitational instability, it is proposed that baroclinic instabilities “neutralize” the atmosphere. In the framework of the two-layer model, the instabilities are thought of as preventing the isentropic slope from increasing beyond the critical slope provided by Phillip’s criterion. The similarity of the observed mid-tropospheric isentropic slopes poleward of the subtropical jet to this critical slope has been taken as confirmation of the basic idea.

The natural procedure for constructing the analogous neutralized state in a continuously stratified atmosphere is to satisfy the Charney–Stern criterion by destroying the temperature gradient at the surface and by destroying the potential vorticity gradient in a layer adjacent to the surface so as to avoid destabilizing vertical curvature at the top of the layer (Lindzen and Farrel, 1980; Held, 1982). In this continuous case it is considerably more difficult to argue that the eddies are successful in neutralizing the flow, since this state bears no particular resemblance to the observed mean flow. Is the aforementioned agreement between the two-layer model’s critical isentropic slope and the observed extratropical slope simply a coincidence?

When the isentropic slopes in Charney’s continuously stratified model drop below the critical slope in the two-layer model, the horizontal wavelengths and vertical scale of the unstable modes begin to decrease. One possibility then is that these small eddies are relatively inefficient at mixing, so that the flow is effectively neutralized if the isentropic slopes drop much below this point (Held, 1978). Because the changes in eddy scales as the mean flow parameters change are quite gradual, however, this argument does not seem adequate. Alternatively, one can use radiative–convective models of the vertical temperature profile (Manabe and Wetherald, 1967) to show that for any reasonable tropospheric static stability the dynamic heating of the troposphere must extend at least a scale height from the surface. One can then argue that an atmosphere dominated by shallower eddies is inconsistent; the static stability would decrease until deeper eddies were generated that could maintain a consistent radiative–convective equilibrium, and this requires isentropic slopes at least comparable to the two-layer model’s neutralizing slope. [See Branscome (1983) and Gutowski (1985) for related arguments.]

In light of all of these untested speculations, it is probably wise to retreat and to ask how well the baroclinic adjustment concept or other closure ideas explain the results from idealized numerical models. A logical starting point might be a two-layer model with radiative relaxation toward a baroclinically unstable temperature gradient, Ekman pumping in the lower layer, and scale-selective horizontal mixing to accept the enstrophy cascade. For what range of radiative equilibrium temperature gradients, widths of the unstable region, and radiative and frictional relaxation times is baroclinic adjustment a useful concept? Are mixing length ideas useful when the meridional width of the unstable region is large compared with the radius of deformation, as argued in Haidvogel and Held (1980)? Under what conditions does a “life-cycle” experiment (in which one finds the most unstable modes on the time-averaged flow, then initializes with the mean flow plus a small amplitude normal mode, and watches the mode equilibrate) provide useful information about the statistically steady state? At what point do multiple zonal

jets emerge as the unstable region is widened [see Williams's (1978) Jupiter simulations]? How does the partition of the enstrophy dissipation between small-scale mixing and large-scale damping (radiative relaxation, Ekman pumping) depend on the various model parameters? Careful numerical experiments aimed at questions such as these are needed if we are to make progress on the difficult eddy flux closure problem, even if results for such an idealized, dry, two-layer model are not directly relevant to the atmosphere.

5. STATIONARY EDDIES AND THEIR INTERACTION WITH TRANSIENTS

5.1. *Extratropical Stationary Eddies*

Given all of these obstacles standing in the way of an adequate theory for the climate of an atmosphere with zonally symmetric lower boundary, it may seem presumptuous to consider an atmosphere with as complex a lower boundary as the Earth's. However, much progress can be made by considering the zonal-mean flow as given and analyzing the deviations from zonal symmetry in the context of linear wave theory. Indeed, the pioneering work of Charney and Eliassen (1949) and Smagorinsky (1953) on topographic and thermal forcing, respectively, held out the promise that linear stationary wave theory might be of quantitative as well as qualitative value in explaining the asymmetries. The goal of a quantitative theory receded somewhat for a number of years, as the calculations became more detailed but did not improve systematically. In retrospect, this seems to have been due to the fact that nearly all calculations were performed on a mid-latitude beta-plane with reflecting walls, thus seriously distorting the meridional propagation of planetary waves and introducing potentially unphysical resonances. More recent work with linear primitive equation models on the sphere has again raised the possibility of quantitatively useful linear theories.

Linear inviscid stationary wave theory breaks down in low latitudes, where the phase speed of the wave (zero) is comparable to the zonal flow speed. There is little doubt that this breakdown results in at least partial absorption. The simplest indication of this is that the stationary eddy momentum flux is nearly always directed from low latitudes to mid-latitudes. Assuming that the theory of planetary waves on a slowly varying basic state is relevant, this immediately translates into the statement that the equatorward propagating waves are of larger amplitude than any poleward propagating waves. While partial reflections are a possibility, as suggested by steady-state nonlinear theories, we are aware of no observational studies that indicate that reflection is occurring in the troposphere; indeed, it will take a careful analysis to distinguish between a reflected wave and a wave forced directly by

tropical heating or, perhaps, by convection generated by the incident wave. It seems to us to be the appropriate working hypothesis that low-latitude absorption is sufficient to prevent stationary wave resonance. This leads us to the position that most of the work on multiple equilibria for stationary waves interacting with zonal flows, depending as it does on resonantlike behavior of the stationary waves, is not likely to be applicable to the troposphere, unless the zonal winds happen to be configured in such a way that they do not allow propagation into the tropics.

An additional problem that stands in the way of quantitative tests of linear stationary wave theory is our lack of information on the observed diabatic heating distribution. One way of trying to circumvent this difficulty is to use the heating distribution produced by a GCM and compare the resulting stationary waves with those produced by the same GCM. Figure 8 shows one result from a study of this sort carried out by Nigam (1983) and Nigam *et al.* (1986). It compares the deviations from zonal symmetry of the 300-mb meridional velocity predicted by a linear model with that produced by the GCM for the Northern Hemisphere winter. A large Rayleigh friction is introduced in the tropics of the linear model to make it strongly absorbing. This damping not only absorbs the waves incident on the tropics, but also controls the strength of the response (both tropical and extratropical) to the tropical diabatic heating. The results are reasonably good at this level, some of the more serious discrepancies being off the west coast of North America and in the immediate vicinity of the Tibetan plateau. The solution deteriorates significantly in extratropical latitudes as one moves to lower levels. The value of such a linear simulation of the stationary wave field is that it can be easily dissected into the responses to different parts of the forcing. Such a dissection shows that the response in the Northern Hemisphere extratropical upper troposphere during winter is a rather complicated superposition of the response to extratropical diabatic heating (mainly latent heating in the oceanic storm tracks), tropical latent heating, and flow over the major mountain complexes, the last being dominant in the meridional velocity and geopotential height field, but with all three of importance for the zonal wind maximum off Japan.

We should not expect too much from linear theory. Transient eddy heat fluxes undoubtedly grow in importance as one approaches the surface. At 850 mb in NH winter, they damp the standing eddy temperature variance with an e-folding time of ≈ 5 days (Lau, 1979). Furthermore, observational studies of the vorticity budget indicate that transient eddy fluxes are as important as the mean fluxes of vorticity in balancing the vorticity loss at the surface in the Aleutian and Icelandic lows (Lau, 1979). In the upper troposphere, on the other hand, linear theory may be better than one might expect at first glance. In quasi-geostrophic theory, for a linear stationary wave in a

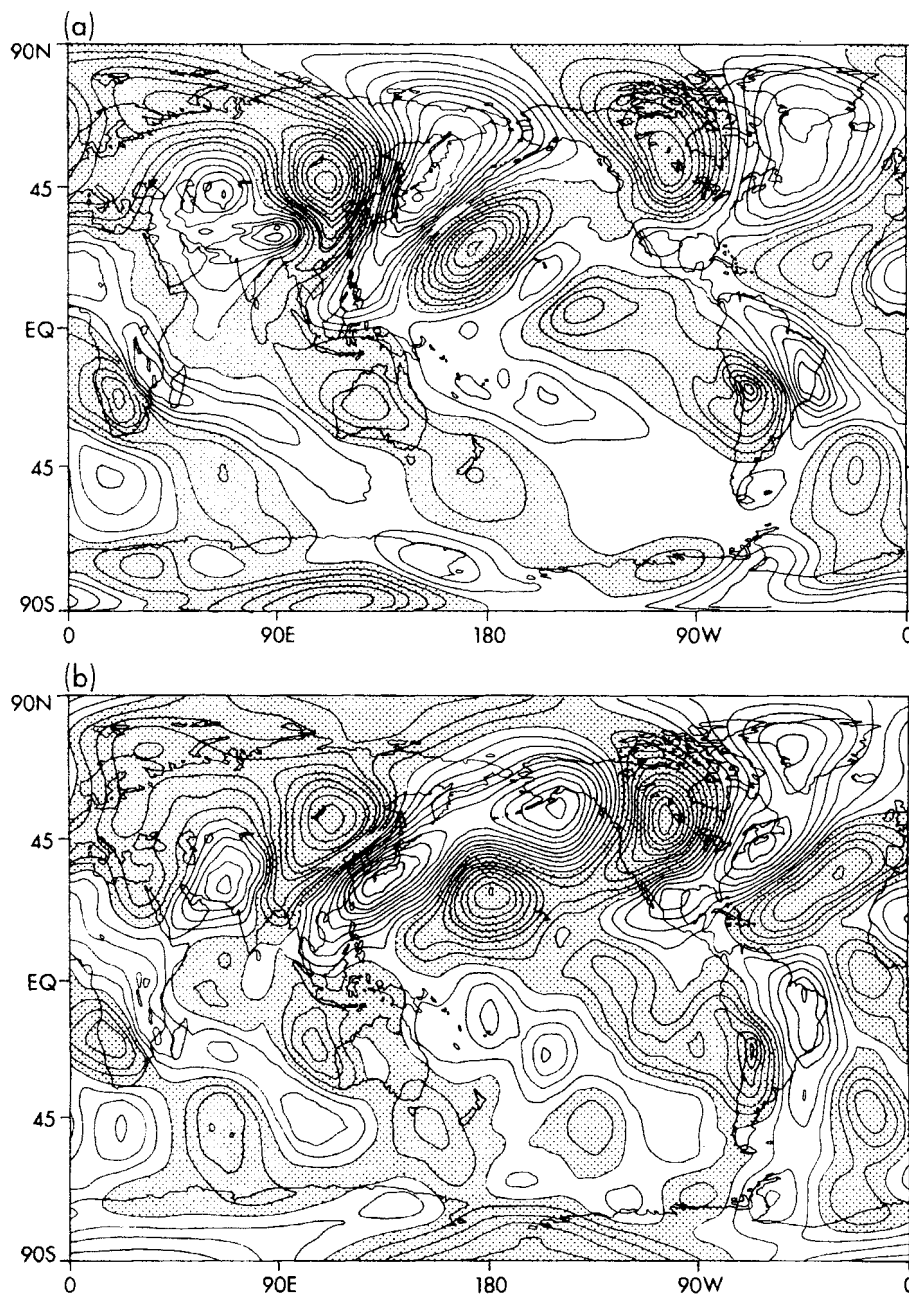


FIG. 8. Deviation of 300-mb meridional velocity from its zonal mean in (a) the linear stationary wave model of Nigam *et al.* (1986), which utilizes the GCM's zonal flow and diabatic heating field and (b) a GCM simulation of NH winter. Contour interval is 1 m s^{-1} and shaded areas are negative.

source-free region,

$$\bar{u} \frac{\partial q'}{\partial x} = -v' \frac{\partial \bar{q}}{\partial y} \quad (5.1)$$

In the special case that \bar{u} and $\partial \bar{q}/\partial y$ are independent of y (but with arbitrary z dependence), we have $J(\psi', q') = 0$, implying that the linear solution satisfies the fully nonlinear equation. If $\bar{u}^{-1} \partial \bar{q}/\partial y$ is slowly varying, $J(\psi', q')$ will be nonzero but still much smaller than a naive scaling would indicate. Perhaps the deterioration of the forced wave solution as one descends in the troposphere is in part a consequence of diabatic heating and transient eddy fluxes destroying the balance (5.1) and thereby creating nonnegligible mean-flow nonlinearity.

5.2. Tropical Stationary Eddies

Progress in developing an understanding of large-scale stationary eddies in the tropics has been slowed by a variety of problems: the absence of a strong mean zonal flow about which to linearize, uncertainty as to the importance of small-scale momentum transport, and the absence of adequate observations. To help focus the discussion, we begin by considering the following steady vorticity, divergence, and thermodynamic equations, which have been linearized about a uniform zonal flow \bar{u} :

$$\bar{u} \frac{\partial \zeta'}{\partial x} + \beta v' = -f D' \quad (5.2)$$

$$f \zeta' - \beta u' = \nabla^2 \phi' \quad (5.3)$$

$$\bar{u} \frac{\partial^2 \phi'}{\partial x \partial z} + N^2 w' = Q' \quad (5.4)$$

We denote the characteristic length scales in the zonal, meridional, and vertical directions by L_x , L_y , and H . The other relevant length scales are $L_\beta = (\bar{u}/\beta)^{1/2}$ and the Rossby radius of deformation $L_R = NH/f$, where we take $f \approx \beta L_y$. Consistent with observations we assume that $L_\beta \approx L_y \ll L_x$. The vorticity equation then gives $\zeta'/D' \approx L_x/L_y$. In (5.3) the advection of divergence is found to be negligible, and this equation gives $\phi' \approx \beta L_y^3 \zeta'$. Finally, taking $w' \approx D'H$, the ratio of horizontal to vertical advection terms in (5.4) is found to be $f^2 L_\beta^2 / (N^2 H^2) = L_\beta^2 / L_R^2$. For tropical motions with $f \approx 2 \times 10^{-5} \text{ s}^{-1}$, $L_\beta \approx 500 \text{ km}$, $N^2 \approx 10^{-4} \text{ s}^{-2}$, and $H \approx 5 \text{ km}$, this ratio is equal to $1/25$ so that the horizontal advection of temperature is negligible. We are left with the interesting situation that the thermodynamic equation gives the divergent flow (assuming that Q is given), the vorticity equation

then gives the rotational flow, and the divergence equation determines the temperature structure.

From the Southeast Asian summer monsoon data of Krishnamurti (1971), Holton and Colton (1972) found that (5.2) was totally unable to model the correct position of the upper-level Tibetan anticyclone unless strong damping of vorticity was included, thereby moving this anticyclone from west of the upper-level divergence (as implied by $\beta v \approx -fD$) to almost coincident with it. This addition of strong vorticity damping has proven to be quite useful in constructing qualitative linear models of the zonally asymmetric mean tropical flow [e.g., Gill (1980)]. The possibility that this upper-tropospheric “damping” is crudely accounting for neglected nonlinearity is, we believe, strongly supported by the analysis of a GCMs tropical vorticity budget (Sardeshmukh and Held, 1984) and the vorticity budget of observed, analyzed, and initialized fields routinely constructed at ECMWF (Sardeshmukh and Hoskins, 1984). The GCM had no sub-grid-scale vertical mixing of momentum in the upper troposphere and a biharmonic horizontal diffusion had little effect on the vorticity budget, and yet the model produced a fairly realistic Tibetan anticyclone and monsoonal rainfall. The vorticity balance was found to be strongly nonlinear, with horizontal advection of relative vorticity playing the dominant role in balancing the stretching. A problem with the GCM analysis was that terms in the vorticity budget averaged over one month had considerable structure on the smallest scales resolved by the model, particularly near the Tibetan plateau. The ECMWF-analyzed fields for the anomalous El Niño – Southern Oscillation NH winter of 1982–1983 used by Sardeshmukh and Hoskins were considerably smoother, but the conclusion as to the importance of nonlinearity was the same.

Important features of the upper-tropospheric vorticity balance are well illustrated by the 150-mb absolute vorticity, divergence, and stream-function contours for the more normal NH winter of 1983–1984, shown in Fig. 9. The simplest balance, $\beta v = -fD$, is clearly inadequate. The regions of strong convection with large $D > 0$ (indicated by stippling) tend to be associated with small absolute vorticity ζ_a , so the generation of anticyclonic vorticity $\zeta_a D$ is smaller than would be obtained from the linearization fD . Comparison of the mean stream function with the mean vorticity suggests that outside regions of intense convection, vorticity is nearly conserved following the flow. Twisting and vertical advection are found to be negligible, and transient terms are generally smaller than the mean flow terms, although not entirely negligible. The relatively small residual found in the budget does not suggest the presence of large friction in the tropical upper troposphere.

The foregoing discussion suggests that a useful model of the tropical

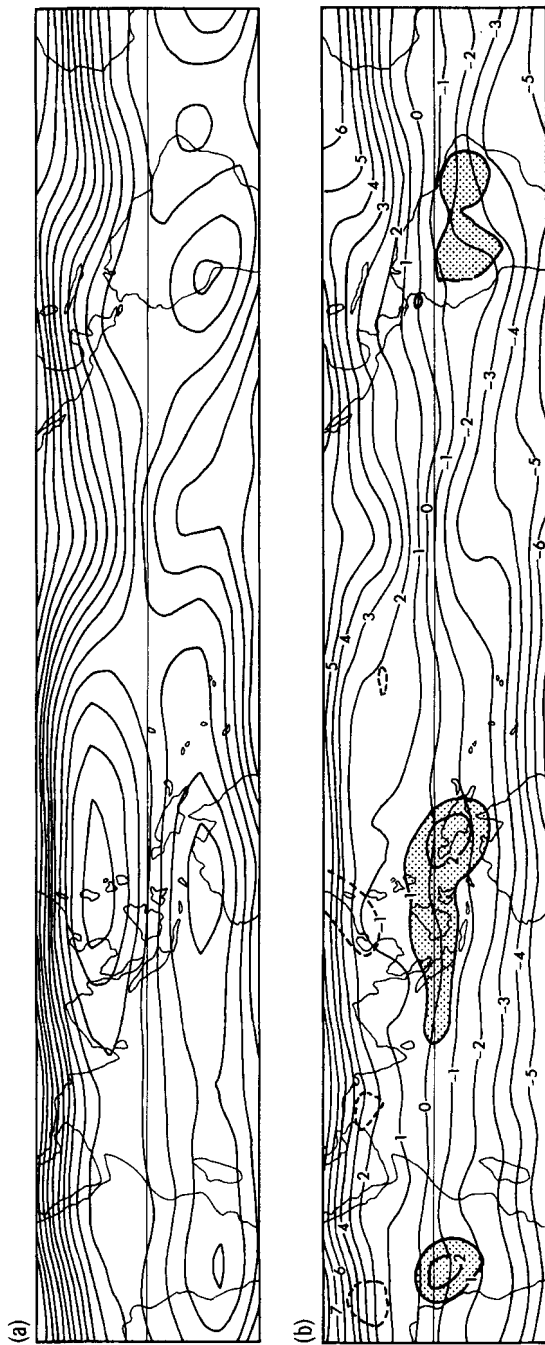


FIG. 9. Contours of (a) stream function and (b) absolute vorticity in the latitudinal belt 30°S to 30°N at 150 mb for the northern winter (DJF) of 1983–1984. The contour intervals are $5 \times 10^6 \text{ m}^2 \text{ s}^{-1}$ and $1 \times 10^{-5} \text{ s}^{-1}$, respectively. Also shown by heavy contours in (b) is the divergence, with a contour interval of $3 \times 10^{-6} \text{ s}^{-1}$. Positive values greater than 3×10^{-6} are stippled and negative contours are dashed.

upper-tropospheric, long-wave pattern corresponding to specified heat sources is

$$\frac{\partial \zeta_a}{\partial t} + \nabla \cdot (\mathbf{v} \zeta_a) = 0 \quad (5.5)$$

Here $\mathbf{v} = \mathbf{v}_\zeta + \mathbf{v}_D$, where \mathbf{v}_D is the specified divergent wind associated with $D = \partial(Q/N^2)/\partial z$. Advection by the divergent flow \mathbf{v}_D is essential; otherwise an anticyclonic vorticity source within a closed stream-function contour of the Tibetan anticyclone, say, could only be balanced by transients or dissipation. Determination of Q is the remaining formidable problem. It should be noted that if the entire Q field is specified, then the flow field at a given level can be determined independent of the flow at other levels. However, in a simple tropical model, one should at a minimum write $Q = Q_{\text{convective}} - T/\tau$ (separating latent heat release from radiative cooling) so as to allow the model to predict the pattern of downward motion that compensates the ascent in the convective regions. The dependence of the radiative cooling on $T\alpha \partial\phi/\partial z$ provides vertical coupling and thereby greatly complicates the problem.

While nonlinearity in the vorticity equation evidently plays a dominant role in the tropical upper troposphere, near the ground the flow is weaker due to surface friction, and the balance appears to be

$$\beta v \approx -fD - \kappa \zeta \quad (5.6)$$

where, once again, $\mathbf{v} = \mathbf{v}_\zeta + \mathbf{v}_D$ with \mathbf{v}_D determined by the heating; the final term represents the effects of stresses in the planetary boundary layer. Both evaporation and moisture transport are strongly controlled by the low-level flow, so one can conceive of estimating $Q_{\text{convective}}$ without reference to the nonlinear upper-tropospheric flow. However, it seems that the pattern of radiative cooling and the low-level divergence field outside of the convecting regions must be affected by the upper-level nonlinearity.

5.3. Zonally Asymmetric Transients

All transient eddy statistics of interest (heat, momentum, and moisture fluxes, eddy kinetic energies, etc.) are observed to be strongly zonally asymmetric. The ‘‘synoptic-scale’’ transients, in particular, are organized into well-defined storm tracks that tend to be located downstream and poleward of the mean jet maxima. Frederiksen’s (1979, 1980) calculations have shown that storm track position can be understood to first approximation from the baroclinic instability of the time-mean zonally asymmetric flow. Thus, it appears that the asymmetry of the lower boundary controls the storm tracks

through its control of the stationary eddy pattern and not primarily through direct thermal or orographic forcing. In particular, "lee-cyclogenesis" (which we take to refer to the direct interaction of cyclones and topography) may be of importance in some regions but does not seem to be an important cause of the major oceanic storm tracks. Based on these instability analyses and observational studies such as that of Hoskins *et al.* (1983), a three-dimensional extension of the baroclinic wave life cycle described in Section 3 is suggested: wave activity is generated by baroclinic instability at low levels off the east coasts of the NH continents, propagates downstream and vertically to upper-tropospheric levels, and then propagates equatorward into regions where the wave activity is dissipated.

The effects of transient eddies on the time-mean zonal asymmetries in mid-latitudes is a complex problem, many facets of which have yet to be explored. Budget studies [i.e., Lau (1979)] indicate a rather modest (but not negligible) role for transient eddies in the structure of the upper-tropospheric stationary waves, and the simulation of a GCMs stationary eddies with a linear model by Nigam *et al.* (1986) seems to confirm this for the NH winter. (We are thinking here of the zonal-mean flow as being given; the transients do exert strong control of the upper-tropospheric wave pattern through their control of the zonal-mean flow on which the waves propagate and of the low-level zonal winds that determine the strength of the orographic forcing.) At lower levels, thermal damping of stationary waves by transients is substantial, and the combined effect of the heat and vorticity fluxes in the storm tracks is to accelerate the low-level westerlies at the start and middle of the track and generate cyclonic (anticyclonic) vorticity north (south) of these westerlies (Lau and Holopainen, 1984; Hoskins *et al.*, 1983). Thus, the transients do appear to help maintain the Icelandic Low–Azores High couplet, as an example. Upstream of these vorticity centers, the low-level equatorward flow of cold continental air and the poleward flow of moist subtropical air have a frontogenetic effect, increasing the low-level baroclinicity in the storm track. The implication is that transients may feed back positively onto their organization into storm tracks. Direct calculations of the effects of the observed transients on linear stationary wave models have been performed by Youngblut and Sasamori (1980) and Opsteegh and Vernekar (1982).

Examination of the wind or temperature tendencies due to observed transients can be misleading. In particular, the effects of transients can be very nonlocal. As an example, consider the idealized situation in which transient mixing is confined to a small region through which pass mean streamlines that then traverse a much larger region where the mean flow is conservative; mixing in the localized region can set the value of potential vorticity conserved along each streamline in the larger region and thereby control the

structure of the flow. As another extreme example, one can conceive of transients as diffusively mixing some quantity (potential vorticity, say) so as to effectively destroy any gradients in some region; but once the gradients have been destroyed, the transient diffusive fluxes of that quantity also disappear. While the role of transients would be clear as one watched the flow evolve toward equilibrium, a budget analysis of the final steady state would not provide this information. These examples are meant only to emphasize that the effects of transient eddies must be studied in the context of a consistent mean flow dynamics.

There are also circumstances in which the formal separation between the time-mean flow and transient eddies itself obscures the underlying dynamics. Consider an atmosphere that cools at the rate $Q(y) = \mu y$, $0 \leq y \leq L$, and suppose that our idealized thermodynamic equation reads

$$\frac{\partial \Theta}{\partial t} = -v \frac{\partial \Theta}{\partial y} - Q \quad (5.7)$$

Let the meridional velocity v be zero except for short bursts in which a uniform southerly wind $V > 0$ advects air poleward. Let T be the interval between bursts and $\tau \ll T$ the duration of a burst, and set $V = L/\tau$ so that by the end of each burst the atmosphere from $y = 0$ to L is nearly isothermal. The time-mean temperature gradient will then be $\approx -\mu T/2$, and the time-mean flow $V\tau/T = L/T$, implying a warming due to this mean flow of $\approx \mu L/2$. Therefore, at $y = L$ the diabatic cooling μL is half balanced by mean heating and half by transients. At $y = 0$, on the other hand, the diabatic cooling is zero, and the mean flow heating $\mu L/2$ is balanced by transient cooling. One is tempted to deduce from this formally correct analysis that the mean flow is the important ingredient in maintaining the warmth in the region, an inference totally at variance with the underlying dynamics. In order to understand the time-mean temperature gradient in such a system, one might try to understand what controls the time interval T between bursts rather than to focus on the transient eddy flux as the quantity of prime interest.

Whether or not analogs of this last scenario are of relevance to the stationary eddy pattern, it does seem suggestive of problems encountered in analyses of blocking episodes in terms of a time-mean (or low-pass-filtered) flow and higher-frequency transients. Conventional analyses of this sort in Hoskins *et al.* (1983) and later unpublished work almost always show the vorticity flux convergence associated with synoptic eddies to be in the direction of increasing the anomalous vorticity in the block; however, the heat flux convergence does not usually appear to be in the right sense. This does not agree with synoptic experience, which is that the poleward flux of warm air ahead of elongated cold fronts seems to reamplify blocks. The example

discussed in the preceding paragraph suggests that this contradiction may be only apparent, the confusion resulting from the inclusion in the mean flow of part of the synoptician's "transience."

Despite the many potential pitfalls, we are optimistic that the developing cross-fertilization among theory, numerical general circulation modeling, and observational studies will result in rapid advances in our understanding of the large-scale flow in the atmosphere. While we do not expect this understanding to be readily translatable into closure schemes and simple models that could usefully compete with GCMs in simulating the time-mean flow in the atmosphere, the most important test of our understanding will remain the ability to distinguish between the essential and the inessential and thus to model aspects of the general circulation in as simple a way as possible.

ACKNOWLEDGMENTS

We would like to thank Peter Phillips and Steve Lyons of the GFDL for assisting with some of the calculations described herein. The influence of Prashant Sardeshmukh and Michael McIntyre on some of the ideas presented here is also gratefully acknowledged. The former also produced Fig. 9 from ECMWF data.

REFERENCES

- Andrews, D. G., and McIntyre, M. E. (1976). Planetary waves in horizontal and vertical shear: The generalized Eliassen-Palm relation and mean flow acceleration. *J. Atmos. Sci.* **33**, 2031–2048.
- Branscome, L. E. (1983). A parameterization of transient eddy heat flux on a beta-plane. *J. Atmos. Sci.* **40**, 2508–2521.
- Chang, C.-P. (1977). Some theoretical problems of the planetary scale monsoons. *Pure Appl. Geophys.* **115**, 1087–1109.
- Charney, J. G., and Eliassen, A. (1949). A numerical method for predicting the perturbations of the middle latitude westerlies. *Tellus* **1**, 38–54.
- Edmon, H. J., Jr., Hoskins, B. J., and McIntyre, M. E. (1980). Eliassen-Palm cross-sections for the troposphere. *J. Atmos. Sci.* **37**, 2600–2616; see also corrigendum: *Ibid.* **38**, 1115 (1981).
- Frederiksen, J. S. (1979). The effects of long planetary waves on regions of cyclogenesis: Linear theory. *J. Atmos. Sci.* **36**, 195–204.
- Frederiksen, J. S. (1980). Zonal and meridional variations of eddy fluxes by long planetary waves. *Q. J. R. Meteorol. Soc.* **106**, 63–84.
- Gill, A. E. (1980). Some simple solutions for heat-induced tropical circulations. *Q. J. R. Meteorol. Soc.* **106**, 447–462.
- Gutowski, W. J., Jr. (1985). A simple model for the interaction between vertical eddy heat fluxes and static stability. *J. Atmos. Sci.* **42**, 346–358.
- Haidvogel, D. B., and Held, I. M. (1980). Homogeneous quasi-geostrophic turbulence driven by a uniform temperature gradient. *J. Atmos. Sci.* **37**, 2644–2660.

- Held, I. M. (1978). The vertical scale of an unstable baroclinic wave and its importance for eddy heat flux parameterization. *J. Atmos. Sci.* **35**, 572–576.
- Held, I. M. (1982). On the height of the tropopause and the static stability of the troposphere. *J. Atmos. Sci.* **39**, 412–417.
- Held, I. M., and Hou, A. Y. (1980). Nonlinear axially symmetric circulations in a nearly inviscid atmosphere. *J. Atmos. Sci.* **37**, 515–533.
- Holton, J. R., and Colton, D. E. (1972). A diagnostic study of the vorticity balance at 200 mb in the tropics during northern summer. *J. Atmos. Sci.* **29**, 1124–1128.
- Holton, J. R., and Lindzen, R. S. (1972). An updated theory of the quasi-biennial cycle of the tropical stratosphere. *J. Atmos. Sci.* **29**, 1076–1080.
- Hoskins, B. J. (1983). Modelling of the transient eddies and their feedback on the mean flow. In “Large-Scale Dynamical Processes in the Atmosphere” (B. J. Hoskins and R. Pearce, eds.), pp. 169–199. Academic Press, New York.
- Hoskins, B. J., and McIntyre, M. E. (1986). In preparation.
- Hoskins, B. J., James, I. N., and White, G. H. (1983). The shape, propagation, and mean flow interaction of large-scale weather systems. *J. Atmos. Sci.* **40**, 1595–1612.
- Hou, A. Y. (1984). Axisymmetric circulations forced by heat and momentum sources: a simple model applicable to the Venus atmosphere. *J. Atmos. Sci.* **41**, 3437–3455.
- Krishnamurti, T. N. (1971). Observational study of the tropical upper troposphere motion field during the Northern Hemisphere summer. *J. Appl. Meteorol.* **10**, 1066–1096.
- Lau, N. C. (1979). The observed structure of tropospheric stationary waves and the local balances of vorticity and heat. *J. Atmos. Sci.* **36**, 996–1016.
- Lau, N. C., and Holopainen, E. O. (1984). Transient eddy forcing of the time-mean flow as identified by geopotential tendencies. *J. Atmos. Sci.* **41**, 313–328.
- Lemone, M. A. (1983). Momentum transport by a line of cumulonimbus. *J. Atmos. Sci.* **40**, 1815–1834.
- Lindzen, R. S., and Farrell, B. (1980). The role of the polar regions in global climate; and a new parameterization of global heat transport. *Mon. Weather Rev.* **108**, 2064–2079.
- McIntyre, M. E., and Palmer, T. N. (1984). The “surf zone” in the stratosphere. *J. Atmos. Terr. Phys.* **46**, 825–850.
- Manabe, S., and Wetherald, R. T. (1967). Thermal equilibrium of the atmosphere with a given distribution of relative humidity. *J. Atmos. Sci.* **24**, 241–259.
- Manabe, S., Hahn, D. G., and Holloway, J. L. (1974). The seasonal variation of the tropical circulation as simulated by a global model of the atmosphere. *J. Atmos. Sci.* **31**, 43–83.
- Matsuno, T. (1971). A dynamical model of the stratospheric sudden warming. *J. Atmos. Sci.* **28**, 1479–1494.
- Nigam, S. (1983). On the structure and forcing of tropospheric stationary waves. Ph.D. Thesis, Princeton University, Princeton, New Jersey.
- Nigam, S., Held, I. M., and Lyons, S. (1986). Simulation of the stationary eddies in a GCM with a linear model. (In preparation.)
- Opsteegh, J. D., and Vernekar, A. D. (1982). A simulation of the January standing wave pattern including the effects of transient eddies. *J. Atmos. Sci.* **39**, 734–744.
- Pedlosky, J. (1970). Finite amplitude baroclinic waves. *J. Atmos. Sci.* **27**, 15–30.
- Pedlosky, J. (1979). Finite-amplitude baroclinic waves in a continuous model of the atmosphere. *J. Atmos. Sci.* **36**, 1908–1924.
- Plumb, R. A. (1981). Instability of the distorted polar night vortex: A theory of stratospheric warmings. *J. Atmos. Sci.* **38**, 2514–2531.
- Sardeshmukh, P. D., and Held, I. M. (1984). The vorticity balance in the tropical upper troposphere of a general circulation model. *J. Atmos. Sci.* **41**, 768–778.
- Sardeshmukh, P. D., and Hoskins, B. J. (1985). Vorticity balance in the tropics during the

- 1982–83 El-Niño–Southern Oscillation event. *Q. J. R. Meteorol. Soc.* **111**, 261–278.
- Schneider, E. K. (1983). Martian great dust storms: Interpretive axially symmetric models. *Icarus* **55**, 302–331.
- Schneider, E. K., and Lindzen, R. S. (1976). A discussion of the parameterization of momentum exchange by cumulus convection. *JGR, J. Geophys. Res.* **81**, 3158–3160.
- Simmons, A. J., and Hoskins, B. J. (1978). The life cycles of some nonlinear baroclinic waves. *J. Atmos. Sci.* **35**, 414–432.
- Simmons, A. J., and Hoskins, B. J. (1980). Barotropic influences on the growth and decay of nonlinear baroclinic waves. *J. Atmos. Sci.* **37**, 1679–1684.
- Smagorinsky, J. (1953). The dynamical influence of large-scale heat sources and sinks on the quasi-stationary mean motions of the atmosphere. *Q. J. R. Meteorol. Soc.* **79**, 342–366.
- Smagorinsky, J. (1963). General circulation experiments with the primitive equations. I. The basic experiment. *Mon. Weather Rev.* **91**, 99–164.
- Stone, P. H. (1972). A simplified radiative-dynamical model for the static stability of rotating atmospheres. *J. Atmos. Sci.* **29**, 405–418.
- Stone, P. H. (1978). Baroclinic adjustment. *J. Atmos. Sci.* **35**, 561–571.
- Thompson, S. L., and Hartmann, D. L. (1979). “Cumulus friction”: Estimated influence on the tropical mean meridional circulation. *J. Atmos. Sci.* **36**, 2022–2026.
- Williams, G. P. (1978). Planetary circulations. 1. Barotropic representations of Jovian and terrestrial turbulence. *J. Atmos. Sci.* **25**, 1399–1426.
- Yamagata, T. (1976). On trajectories of Rossby wave packets released in a lateral shear flow. *J. Oceanogr. Soc. Jpn.* **32**, 162–168.
- Youngblut, C., and Sasamori, T. (1980). The nonlinear effects of transient and stationary eddies on the winter mean circulation. Part I. Diagnostic analysis. *J. Atmos. Sci.* **37**, 1944–1957.